Geophysical Research Letters

RESEARCH LETTER
10.1029/2020GL088776

Orbital Forcing Strongly Influences Seasonal Temperature Trends During the Last Millennium

Lucie J. Lücke[1], Andrew P. Schurer[1], Rob Wilson[2], and Gabriele C. Hegerl[1]

[1]School of Geosciences, University of Edinburgh, Edinburgh, UK, [2]School of Earth and Environmental Sciences, University of St Andrews, St. Andrews, UK

Key Points:

- Orbital forcing induces a strong seasonal fingerprint in climate model simulations, which is distinct from any other forcings
- Over the last millennium, surface temperature trends simulated by climate models lag asymmetrically behind the insolation by around a month
- Differences between long-term trends of proxy records could be caused by seasonal orbital forcing, which influences climate reconstructions

Supporting Information:

- Supporting Information S1
- Data Set S1
- Data Set S2
- Data Set S3

Correspondence to:
L. Lücke,
lucie.luecke@ed.ac.uk

Citation:
Lücke, L. J., Schurer, A. P., Wilson, R., & Hegerl, G. C. (2021). Orbital forcing strongly influences seasonal temperature trends during the last millennium. *Geophysical Research Letters*, *48*, e2020GL088776. https://doi.org/10.1029/2020GL088776

Received 5 JUN 2020
Accepted 16 DEC 2020

Abstract Insolation changes caused by the axial precession induce millennial trends in last millennium temperature, varying with season and latitude. A characteristic seasonal trend pattern can be detected in both insolation and modeled surface temperature response. In the extratropical Northern Hemisphere, the maximum insolation trend occurs around April/May, while the minimum trend occurs between July and September. The temperature trend lags behind insolation trend by around a month. Hence orbital forcing potentially affects long-term trends in proxy data, which are often sensitive to a distinct seasonal window. We find that tree-ring reconstructions based on early growing season dominated records show different millennial trends from those for late summer dominated proxies. The differential response is similar to that seen in pseudo proxy reconstructions when considering proxy seasonality. This suggests that orbital forcing has influenced long-term trends in climate proxies. It is therefore vital to use seasonally homogeneous data for reconstructing multicentennial variability.

Plain Language Summary The Earth's axis spins like a slightly wobbly gyroscope, with one spin taking around 24,000 years. Depending on the phase of the spin, more or less sunlight comes in during the different seasons, impacting the Earth's climate. This is orbital forcing. Analyzing temperature data produced by global climate models, we found that orbital forcing causes a distinct seasonal trend pattern over the last millennium, which should influence global and regional climate. These patterns are very different from other natural climate forcings-like volcanic eruptions or changes of the Sun's energy output. We have also found evidence of orbital forcing in reconstructions of past climate using natural climate archives such as tree rings and other climate proxies. These findings can potentially resolve previous inconsistencies in long-term climate change found in proxy reconstructions and climate model output.

1. Introduction

It is a unique property of orbital forcing that it can be reconstructed over very long timescales with almost complete certainty, as the variation of the orbital parameters is mathematically well understood. Daily insolation can be precisely calculated on timescales of millions of years (Laskar, 1986, 1988, 2004). However, its influence on the climate system is less certain. The idea that the variation of the orbital parameters influences daily insolation and thus long-term climatic change goes back to the pioneering work of Milankovitch (1941). Since then, orbital forcing has been successfully detected in proxy records on multimillennial timescales and has been attributed to be the cause of glaciation cycles (e.g. Hays et al., 1976; Imbrie et al., 1992). Many other studies have confirmed Milankovitch's theory (see also Alley et al., 2002; Kawamura et al., 2007; Parrenin & Paillard, 2003 Raymo, 1997).

Comparison of model simulations and proxy records have also confirmed that orbital forcing was one of the key drivers of climatic change during the mid to late Holocene (Wanner et al., 2008). Over the last millennium, volcanic forcing was the main driver of natural temperature variability on multidecadal timescales (Lücke et al., 2019; Masson-Delmotte et al., 2013; Neukom et al., 2019; Otto-Bliesner et al., 2016; Schurer, Hegerl, et al. 2013). However, some discrepancies between models and proxies remain. For example climate models seem to underestimate the amplitude of multicentennial variability compared to proxy reconstructions, which could result, for example from model errors (Ljungqvist et al., 2019) or proxy biases (Lücke et al., 2019).

Studies of preindustrial last millennium temperature have repeatedly found negative millennial trends in high latitude proxy data, which coincide with a negative insolation trend caused by orbital forcing. For

example, Kaufman et al. (2009) found a pervasive cooling in high-latitude proxy reconstructions of summer temperature and inferred that it was caused by orbital forcing. McKay & Kaufman (2014) obtained an even higher negative trend in reconstructed annual temperature of the same area, although they questioned the suitability of their reconstruction to determine long-term variability. Esper et al. (2012) found consistent trends around −0.2 to −0.3 K/ky in Scandinavian latewood density (late summer) proxies, in agreement with model data, and attributed these to orbital forcing. However, they could not find similar trends in data based on ring width, and suggested that ring width data could be limited in preserving long-term trends. Phipps et al. (2013) found that simulations which are only subjected to orbital forcing could not replicate the long-term trends previously observed by Esper et al. (2012) and Kaufman et al. (2009) for global annual mean temperature. They suggest that seasonal or geographical biases in proxy reconstructions could potentially be responsible for the larger trends, as proxy reconstructions tend to be more representative of higher latitudes and some records are biased toward summer. They obtained stronger long-term trends in their simulations, when taking these biases into account.

Klippel et al. (2020) investigated the magnitude of the trend displayed by proxy records and their inherent large-scale properties including latitude (mid vs. high) or seasonal sensitivity (summer vs. annual temperature), but found no significant relationship. However, they found that millennial trends in ice cores, marine, and lake sediments were stronger than in tree-rings. This discrepancy between proxy data and model simulations, but also between different types of proxy data, has so far remained unresolved.

While authors have compared mainly tree-ring width against latewood density data, more specific characteristics inherent to the data sources have not been distinguished. In this study, we attempt to group proxy data according to their seasonal sensitivity to find an explanation for the aforementioned discrepancies. The exact seasonality of large-scale proxy reconstructions is often difficult to establish, as data sources with different monthly sensitivity are mixed and the exact seasonal sensitivity of an individual record is uncertain. Most reconstructions of past surface temperatures have been calibrated to either summer (e.g. Anchukaitis et al., 2017; Briffa, 2000; Kaufman et al., 2009; Schneider et al., 2015; Wilson et al., 2016) or annual (e.g. D'Arrigo et al., 2006; Frank et al., 2007; McKay & Kaufman, 2014; Neukom et al., 2019) instrumental temperature data. Esper et al. (2005) found that the target seasonality plays a role for the amplitude of the reconstruction and that amplitudes are higher when scaling to annual temperature compared to summer temperatures. The decreased amplitude for summer could be explained by early instrumental biases (Böhm et al., 2010). Several studies have suggested that reconstructions of seasonal versus annual temperatures are otherwise statistically indistinguishable on multidecadal and longer timescales (Cook et al., 2004; Esper, 2002; D'Arrigo et al., 2006). However, given that tree growth is related to growing season conditions, it was recommended to calibrate tree-ring reconstructions to summer temperature (Wilson et al., 2007, 2016).

In this study, we investigate the effect of the seasonality of insolation trends due to orbital forcing on simulated and reconstructed temperature over the preindustrial last millennium (AD 850–1850). We find that orbital forcing induces a characteristic seasonal trend pattern in climate models, which lags behind the insolation by around a month. In contrast, negative trends arising from other forcings are fairly constant throughout the whole year. A similar seasonal trend pattern is found in proxy reconstructions when accounting for their different seasonal sensitivity, which could be explained by orbital forcing. Our results could not only resolve certain model-proxy discrepancies, but also provide an explanation for discrepancies between different proxy types, such as ring width and density data.

2. Data

2.1. Orbital Data

We use the numerical solutions for the eccentricity e, the climatic precession ψ, and the obliquity ϵ and insolation quantities provided by Laskar et al. (2004). The insolation is given as the monthly mean on a longitudinal grid of 5° resolution. To first order, e and ϵ vary at periods of around 400,000 and 441,000 years (Berger & Loutre, 1991) and are in decline over the entire Holocene (Figure S1). Given their large periodicity, e can be assumed to be approximately constant for our analysis. ϵ is responsible for a small decrease in global annual insolation (around 0.01 W m^{-2}), and introduces a zonal dependence to the millennial insolation trend. In contrast, ψ induces major changes in seasonal insolation on shorter timescales, with a periodicity

of around 24,000 years to first order (Berger & Loutre, 1991). The global seasonal insolation exhibits the same periodicity as the precession, following the precession with different phase shifts.

2.2. Model Data

For the multimodel mean, we use model simulations from six members of the Climate Model Intercomparison Project Phase 5 (CMIP5, [Taylor et al., 2012]), all covering AD 850–2005. We include CCSM4 (Landrum et al., 2013), CESM-LME (Otto-Bliesner et al., 2016), CSIRO-Mk3L-1–2 (Phipps et al., 2011, 2012), GISS-E2-R (Schmidt et al., 2014), MPI-ESM-P (Giorgetta et al., 2013), IPSL-CM5A-LR (Dufresne et al., 2013), and HadCM3 (Schurer, Tett, & Hegerl, 2014). All simulations include volcanic, solar, orbital, and greenhouse gas forcing as prescribed by the Paleoclimate Model Intercomparison Project Phase 3 (PMIP3) (Braconnot et al., 2012; Schmidt et al., 2011, 2012). All but CSIRO also include land-use changes. Simulations from CCSM4, GISS, and IPSL show relatively strong long-term drifts at high latitudes. Thus, we subtract the associated CMIP5 piControl simulation for each model before we calculate long-term trends. All simulations show consistent trend patterns when accounting for those drifts (Figure S2).

We compare these results with single forcing simulations from the CESM-LME. The simulations use a version of CESM-CAM5_CN (1.9 × 2.5_gx1v6), with a resolution of ∼2° in atmosphere and land components and ∼1° resolution in ocean and sea ice components. Besides the 13 simulations including all forcings, we use two unforced control simulations to calculate the model drift and several experiments including single forcings. Given that the drift is very small, we do not subtract it from the simulation before calculating long-term trends. We compare long-term trends from orbital forcing only with the influence of other forcings, calculated as the sum of volcanic, solar, greenhouse gas, and land use/land cover changes (three simulations for each forcing).

2.3. Instrumental Data

For the calibration of the proxy reconstructions, we use CRUTEM4 (Osborn & Jones, 2014), a gridded data set of global historical near-surface air temperature anomalies over land with a resolution of 5° from 1850 to 2015. To avoid biases from insufficient instrumental shielding (Böhm et al., 2010) and poor geographic coverage, we follow Wilson et al. (2016) and exclude data prior to 1880 for calibrating mid-latitudinal data and prior to 1900 for high-latitudinal data. Uncertainty may still arise from varying coverage even for later periods, which decreases toward higher latitudes and is generally higher in Western Europe and North America.

2.4. Proxy Data

2.4.1. Mid Latitudes

In order to reconstruct mid latitudinal temperatures, we use data provided by the Northern Hemisphere Tree-Ring Network Development (N-TREND) consortium as published by Wilson et al. (2016) and Anchukaitis et al. (2017), containing carefully selected high quality tree-ring chronologies and local reconstructions. It includes 54 tree-ring records, from which 11 are derived from ring-width (TRW) measurements, 18 are derived from maximum latewood density (MXD) and 25 are mixed records (MIX). The latter combine reconstructions derived from different measurement methods, such as TRW, MXD, and blue intensity (BI) data. MXD and BI provide similar information on relative wood density (see Björklund et al. (2014); Rydval et al. (2014) for more information). The records vary in length, starting between AD 750 and 1710. Each record has an individual optimal target season, reflecting the trees' growing season, identified by Wilson et al. (2016), correlating the individual records against the local CRU TS 3.2 (Harris et al., 2014) mean temperature grid. The target seasons differ widely, ranging from a single month to several (Figures 1a–1c). We classify the data into two groups: early summer (sensitive up to July) and late summer (sensitive from July onwards). Early summer includes only ring-width and mixed data, while late summer includes width, density and mixed proxies. Given that total ring-width is dominated by earlywood growth, and latewood density type records use only the final cells of the latewood formation (Björklund et al., 2017), our classification is sensible also from a biological point of view.

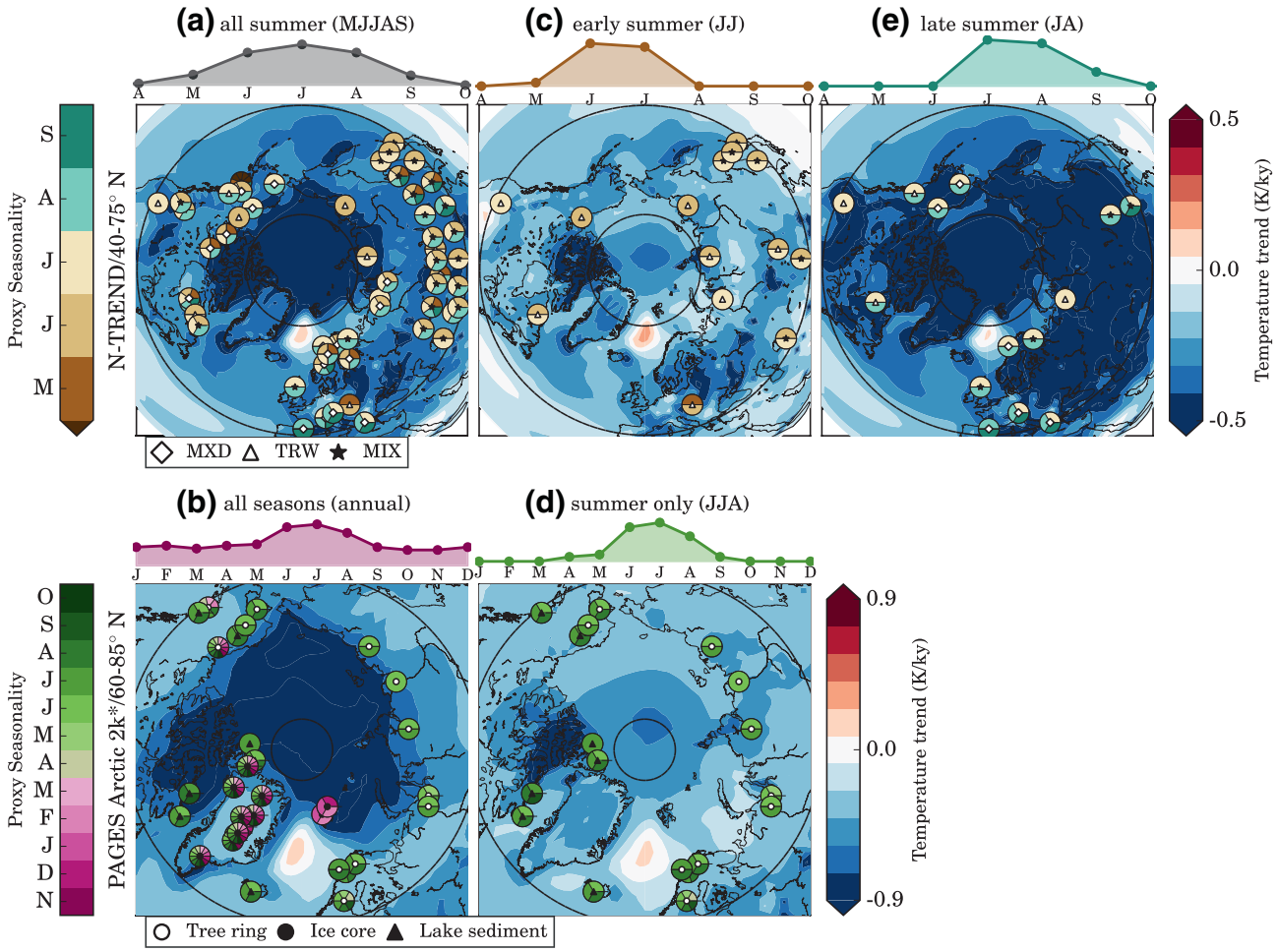

Figure 1. Spatial distribution and seasonal sensitivity of proxy records (top: N-TREND data set [Anchukaitis et al., 2017; Wilson et al., 2016], bottom: annually resolved PAGES Arctic 2k records [McKay & Kaufman, 2014]). (a), (b): full data sets, (c)–(e): seasonally homogeneous subsets. The pie charts denote the seasonal sensitivity of each individual proxy archive as identified by the original publications. On the top of each spatial plot, we show the cumulative seasonality of the respective data sets. The background shading denotes the local temperature trend (AD 850–1850) of the CESM-LME ensemble mean during the target season of each data set.

2.4.2. High Latitudes

We use multiproxy data from the revised PAGES (Past Global Changes) Arctic 2k data set (v1.1.1, McKay & Kaufman (2014)), containing selected and updated records from the first PAGES Arctic 2k database (2k Consortium, 2013). In order to replicate the reconstruction method used for mid latitudinal data, we include only annually resolved data extending into the twentieth century, restricting the data set to 32 proxy records (12 ice cores, 13 tree rings, and 7 lake sediments). We refer to this data as PAGES Arctic 2k*. The data set overlaps with a few tree-ring records from N-TREND, which in some cases contains updated chronologies from PAGES. Based on the seasonal sensitivity stated in the original publications, the data includes 18 summer proxies (JJA), 11 annual, 2 winter (DJF), and 1 February to August proxy. Besides the complete data set, we create an additional seasonally homogeneous subset including all summer records (summer only) (Figures 1d–1f).

3. Hemispheric Temperature from Proxy and Climate Model Data

3.1. Proxy Reconstruction Method

We create an ensemble of hemispheric reconstructions for land surface temperature as in Lücke et al. (2019), based on iterative nesting and scaling to instrumental data (D'Arrigo et al., 2006; Wilson et al., 2016, 2007). We target the mid-latitudinal band between 40 and 75° N for N-TREND, and 60–85°N for PAGES Arctic

2k*. All subsets of N-TREND are calibrated over the period 1880–1988, maximizing data availability of both proxy data and observations. Arctic 2k* subsets are calibrated between 1900 and 1967, reflecting the decreased data availability at higher latitudes.

To gain an estimate of calibration and coverage uncertainty, we vary the calibration period and bootstrap the data set to eventually gain a reconstruction ensemble of 100 ensemble members per data set. In addition to the full calibration period, we split the calibration period for N-TREND into three windows of each 60, 70, and 80 years (40, 50, and 60 for Arctic 2k*). Each reconstruction is again bootstrapped by removing in turn a record from the data set (see Appendix A1 for more detail). For each individual data set, we choose the calibration target season to match the cumulative seasonal sensitivity of the included proxy records.

3.2. Hemispheric Temperature from Climate Model Data

We produce hemispheric timeseries of climate model output using three different methods. First, we use the weighted average of all model grid points within the latitudinal band and within the target season of the proxy reconstructions (CESM full band). We additionally generate a timeseries from the model data sampled at the grid points closest to the proxy locations within the target season of the proxy reconstruction (CESM proxy location). The resulting timeseries closely resembles the full band and uses seasonally homogeneous data. Last, we generate a pseudo proxy reconstruction (PPR), mimicking the heterogeneous seasonal composition of the proxy data and its reconstruction method. For each proxy record, we extract monthly climate model data at the grid point closest to its location, limited to the period at which proxy data is available. We use the monthly average within each proxy record's seasonal sensitivity window. Thus, we obtain a timeseries of model data for each proxy record that reproduces its seasonal characteristics. To concentrate on the aspect of seasonal sensitivity, we have not added noise to the pseudo proxy records, making them perfect representations of modeled climate variability. We replicate the proxy reconstruction method with the resulting pseudo proxy data sets for each model ensemble member, producing a total of 13×100 PPR's for each proxy target data set (see Appendix A2 for more detail).

4. Orbital Forcing and Millennial Trend Patterns in Climate Model Data

The change of the orbital parameters over time induces an insolation trend, which varies with month and latitude (Figure 2). The monthly insolation trend takes the form of a propagating wave, moving forward in the year over the course of the Holocene (top). The signal is strongly zonally dependent, such that at high latitudes maximum and minimum trend are seasonally close together at all periods. During the last millennium, high northern latitudes are expected to experience an increase in insolation during April and May while insolation decreases in July and August. Thus, the magnitude of the trend changes rapidly between May and August. A similar seasonal variation in trends occurs at high southern latitudes. This finding is of particular importance, as proxy data sets are often biased toward both higher latitudes and summer temperature. Thus they directly encompass this highly variable range, as was pointed out by Phipps et al. (2013). This indicates that even small differences in seasonal sensitivity could lead to notable differences between temperature reconstructions.

We find a similar sinusoidal trend signal in globally averaged surface temperature of the last millennium produced by all-forced climate simulations (Figures 3a and 3b). This signal is found in all individual climate models used for our analysis (Figure S3) as well as in CESM simulations including orbital forcing only (Figure 3c). In contrast, other forcings create a negative trend signal, which is approximately constant throughout the year (Figure 3d). The orbital only simulations are the only ones which display a warming trend, which coincides roughly with the period and region of zero trend in the all-forced simulations. Hence the detection of negative millennial temperature trends at high latitudes alone is not sufficient as attribution to orbital forcing as these could be caused by a number of different forcings. Therefore, if we wish to attribute millennial trends to orbital forcing it is the relative seasonal pattern, which is the most important pattern.

Furthermore, we observe that the temperature lags behind the insolation by around one to two months. This can be explained by the thermal inertia due to the high heat capacity of the ocean mixed layer, causing a delayed response of the surface temperature to insolation (Prescott & Collins, 1951). This mechanism

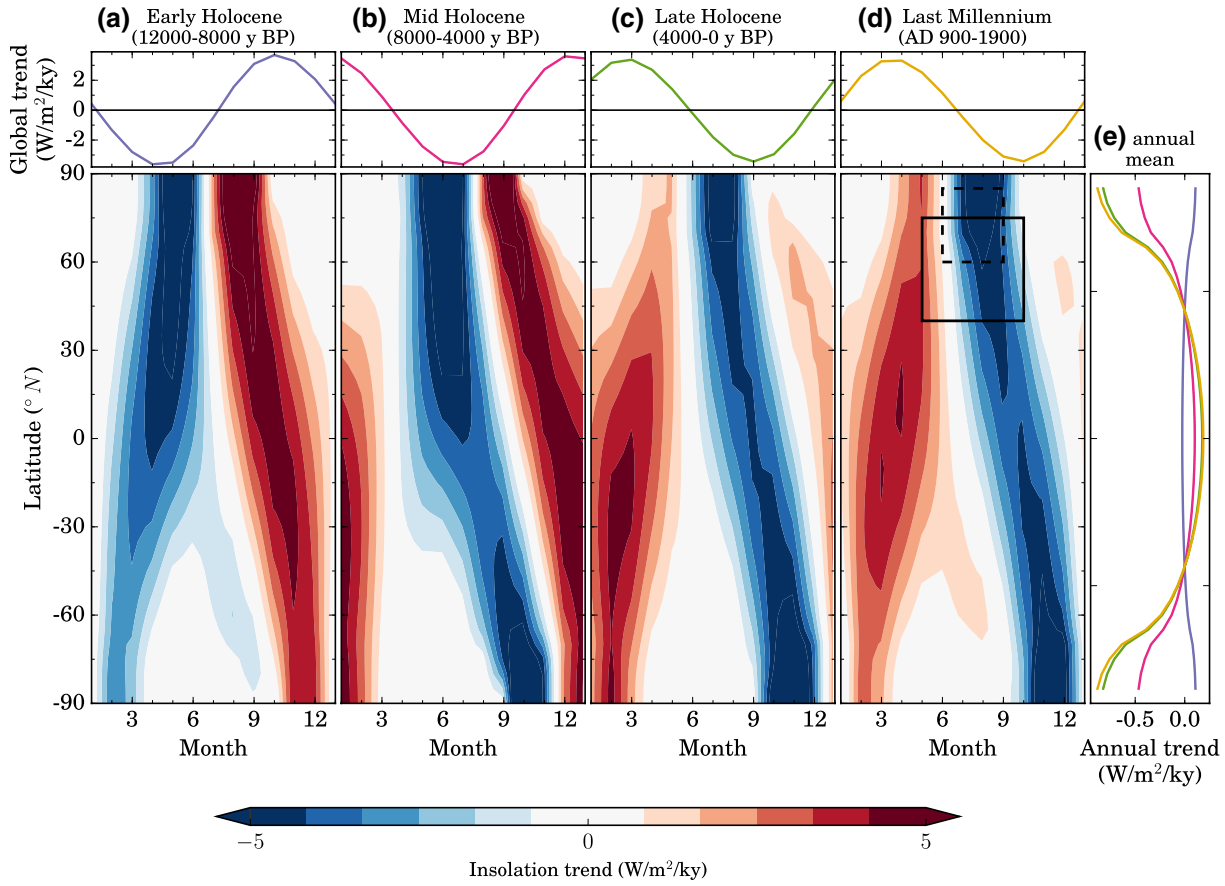

Figure 2. Insolation trend during the Holocene (a–c) and the last millennium (d). The right panel shows zonally resolved annually averaged insolation (e). The zonal and seasonal sensitivity range of N-TREND (Arctic 2k* summer proxies) are shown as a solid (dashed) box in (d).

also explains the larger amplitude of the seasonal trend cycle of land only data. We also note that there is a slight asymmetry in the lag between the minimum and maximum peak trends. A number of seasonally and geographically dependent mechanisms could cause an asymmetry like this (Donohoe et al., 2020). For example, the larger depth of the mixed layer in winter could lead to an increased heat capacity and thus a slower temperature increase in early spring compared to late summer (Bathen, 1972). Other mechanisms could include sea ice cover, which could induce positive or negative feedbacks depending on the season and the sign of the insolation trend (Fischer & Jungclaus, 2011).

The lag of the temperature response behind the forcing has important implications for proxy record trends, which often respond to temperature changes during a narrow seasonal window. In the case of mid-latitudinal tree-ring data, negative temperature trends would only influence proxies, which are sensitive to late summer temperatures (solid box, Figure 3). For higher latitude data, the lag would particularly impact summer proxies (dashed box). This seasonally lagged response to the forcing trend is a key finding of the study and could have important implications, particularly for previous studies, which have compared insolation trends instantaneously with trends found in proxy records (Esper, 2002; Kaufman et al., 2009; Klippel et al., 2020).

5. Millennial Trends in Proxy Reconstructions

We calculate the millennial trends up to AD 1850 in our proxy reconstruction ensembles, varying the start year of the fit to account for changing proxy availability and compared the results with data from CESM simulations (Figures 4a and 4c). In the N-TREND data, we observe a weaker trend for early summer and a stronger trend for late summer data, a pattern which is replicated by the model data. We conclude that the trend pattern in the latter could have been caused by orbital forcing (Figure 4b), as no other forcings

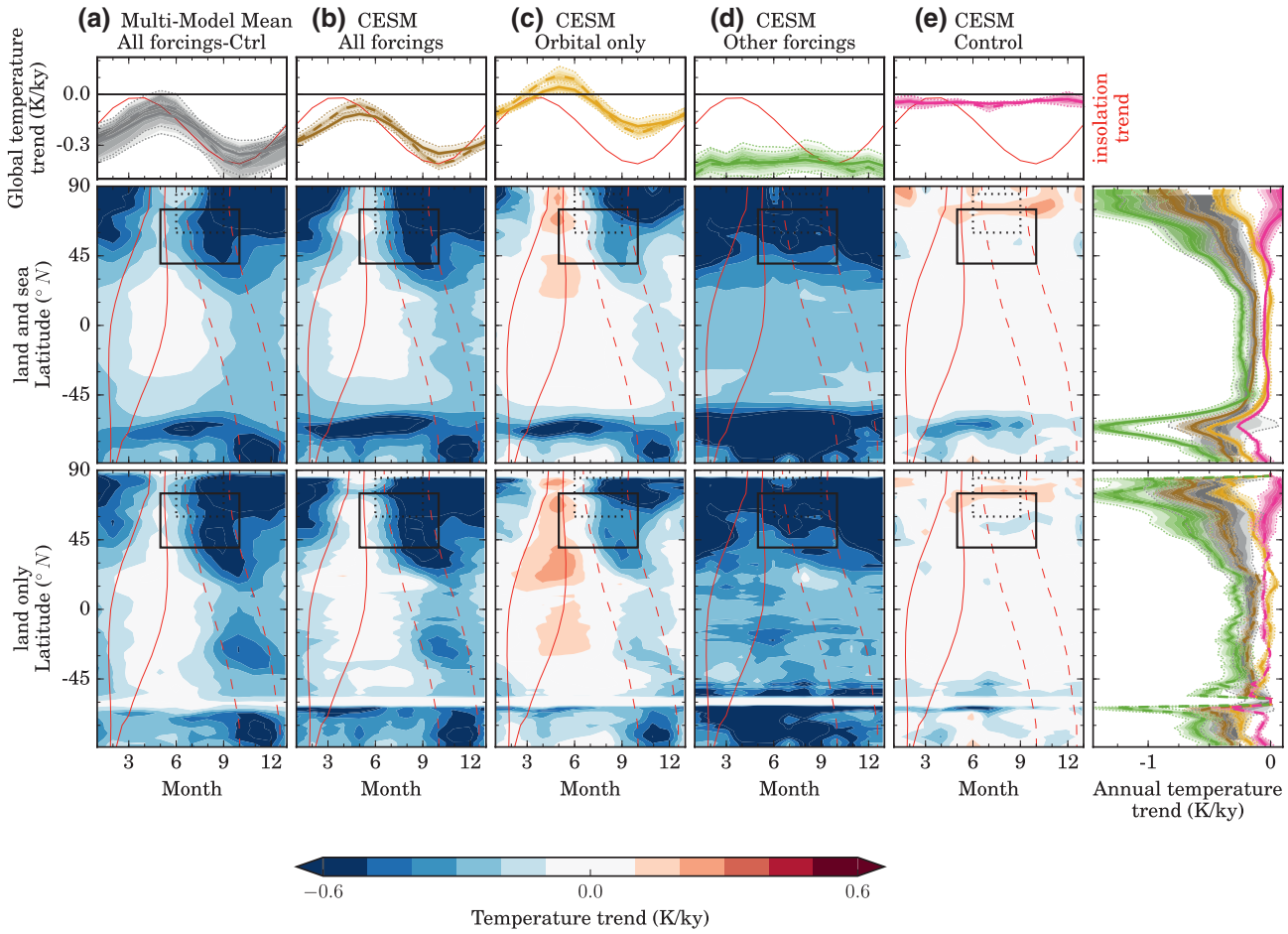

Figure 3. Temperature trends in simulations of last millennium climate (AD 850–1850). (a) Multimodel mean of six climate models minus their control simulation. (b)–(e) Ensemble mean of several CESM-LME experiments. Top: seasonal evolution of the global mean temperature trend of land and sea (solid) and land only (dashed) model data. The millennial insolation trend is included as a red line in the top panels and as a red contour at ±2.5 W/m^2/ky (solid: positive, dashed: negative forcing). The solid (dotted) black box shows the seasonal and zonal sensitivity range of N-TREND (Arctic 2k* summer) proxies.

produce a seasonal difference (see Section 4). The complete proxy data set shows a stronger trend than the seasonal subsets, which is not replicated by the equivalent model data. This could be a result of the data availability or reconstruction method, as the PPR does not conserve the trend difference between late summer and all summer, as observed in the model data. The PAGES Arctic 2k* data are slightly less conclusive. We observe a difference in trend between the complete data set and the summer only data. However, there is no clear orbital forcing pattern detectable in the model data for JJA versus annual temperature. While we expect the trend to be weaker in summer due to the positive orbital forcing, no clear signal can be found when comparing JJA and annual data (Figure 4d) and the model trends overlap widely. There is, however, a significant difference in trend in the proxy reconstruction. While the trend of the summer reconstruction is well in line with the model results, the trend in the complete data set, calibrated to annual data, produces a much stronger trend than found in the model. This could potentially be a result of data quality or availability, remaining seasonal sensitivity in annually calibrated data or the reconstruction method (compare the slightly inflated trends in the PPR).

6. Discussion and Conclusion

Our results from comparing patterns in seasonally restricted proxy reconstructions are promising for attributing seasonal trends to orbital forcing. However, both magnitude and relative difference of the trends found in model data and proxy reconstructions are subject to various uncertainties, which may have influ-

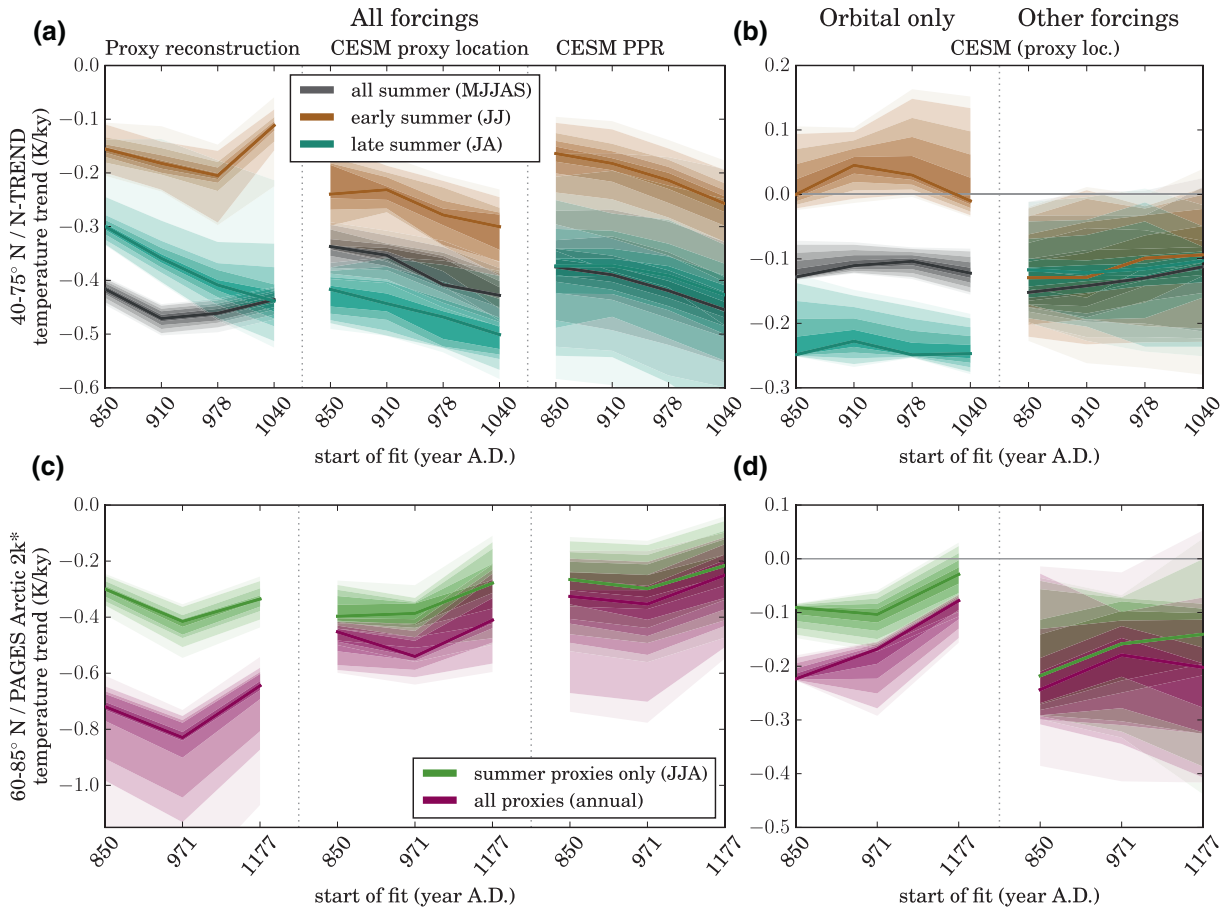

Figure 4. Trends of proxy reconstructions and CESM data up to AD 1850, with varying start year. (a), (c): Reconstructions compared to the model response at proxy locations and the pseudo proxy reconstruction, including all forcings. (b), (d): Model results including orbital forcing only and other forcings. Solid line: median, shading: 60th to 95th percentiles.

enced our results. In the case of the models this includes, for example, model errors and uncertainties in the forced response and internal variability. However, all climate models agree well on the magnitude of the cooling trend as well as the sinusoidal seasonal trend pattern (Figures S6 and S7). Small differences exist regarding the phase shift between insolation and temperature trend, but the models roughly agree on a lag of one month. This robustness of the model results provides a strong theoretical basis for a clear seasonal fingerprint of orbital forcing over the last millennium, which we should expect to see in proxy temperature records over this period.

In the case of the proxy results, we cannot exclude the possibility that the trend pattern in the proxy data is caused by methodological or spectral proxy biases. Methodological biases could arise from the calibration, for example, weaker correlation with instrumental data could suppress the trend (which could be an issue in particular for N-TREND early summer data), but also from detrending methods. It is known that certain detrending methods do not preserve low-frequency variability (Melvin et al., 2012), which could induce a flat bias in the reconstruction. This could in particular influence N-TREND late summer (includes two such records: IDA, KOL, see Table S1), but also early summer (also includes IDA). On the other hand, trends could also be overestimated following detrending – a known issue for at least one record (QUEw) included in N-TREND all and late summer (Anchukaitis et al. (2017)). Furthermore, spectral biases inherent to the proxy data could arise from biological memory processes and overestimate the trend (Lücke et al., 2019). We also cannot exclude the possibility that spectral differences exist between ring-width and latewood density as suggested by Esper et al. (2012), and that our results simply express the characteristics associated with

these datatypes. Limited data availability of the seasonal data sets and potential data quality issues, as well as uncertainties in the seasonal sensitivity could further reduce confidence.

The interpretation of the results is increasingly complicated for inhomogeneous proxy data sets. We notice that for both the N-TREND and especially for the PAGES data set, the trend of the reconstruction including all data differs more from the model than for the seasonally homogeneous data subsets. This applies in particular to the PAGES data set, which includes multiproxy data whose seasonal sensitivity vary strongly. While it is thought that ice-cores and marine/lake sediments may be better than tree rings at capturing low-frequency variability (Esper et al., 2004), the summer reconstruction (tree-rings and lake sediments only) seems to be more in line with the model results. This could reflect how different seasonal proxy characteristics complicate the interpretation of results from multiproxy data, and accordingly decrease our confidence in the results.

We conclude that orbital forcing has likely played a key role in long-term seasonal forcing during the last millennium. While other forcings cause negative millennial temperature trends throughout the year, orbital forcing is the only one inducing a characteristic seasonal fingerprint that may lead to differential millennial cooling across seasons. Thus, negative trends in regional high latitude summer proxy data alone cannot be attributed to orbital forcings as other forcings may also cause negative trends during that time. The trends detected in modeled surface temperature lag behind insolation trends by around a month. Since the period of tree-ring formation encompasses both months of positive and negative orbital trends, trends in tree-ring data will likely depend on their specific seasonal sensitivity. It is therefore critical when interpreting long-term trends in proxy reconstructions to consider the specific seasonal sensitivity of the individual proxy records as well as the lagged relationship between the forcing and the temperature response.

Our analysis shows that climate models and proxy data show similar seasonal trend patterns, which can, in the case of the model data, be attributed to orbital forcing. However, a lack of clearly seasonally resolved, high-quality proxy data makes it impossible to reliably detect orbital forcing in last millennium proxy reconstructions at present, even though differential trends in proxy data suggest an orbital influence.

Our findings could resolve previous data discrepancies, including the difference in long-term trends found in ring width and density data (Esper et al., 2012; Fuentes et al., 2018; Klippel et al., 2020). It also provides an explanation for differing low-frequency variability between proxy reconstructions and model simulations (e.g. the difference between MCA and LIA). We strongly advise against the mixing of proxy data with unknown or differing seasonal sensitivities when it comes to reconstructing long-term trends, or focus on multidecadal variability for such reconstructions (e.g. Neukom et al. (2019)).

Conflict of Interest

The authors declare no conflict of interests.

Data Availability Statement

All model data are publicly available: PMIP/CMIP model output is available via the Earth System Grid at: http://pcmdi9.llnl.gov/. The CESM data can be downloaded from: http://www.cesm.ucar.edu/projects/community-projects/LME/. The CSIRO Mk3L data from: https://www.ncdc.noaa.gov/paleo-search/study/16337. Both proxy data sets are publically available. The N-TREND data set can be downloaded at: https://ntrenddendro.wordpress.com/tr-data/. The PAGES Arctic 2k v1.1.1 can be downloaded from: https://www.ncdc.noaa.gov/paleo-search/study/16973. All data generated or analyzed during this study will be publically available on the University of Edinburgh DataShare server.

Acknowledgments
L. Lücke. was supported by a studentship from the Natural Environment Research Council (NERC) E3 Doctoral training partnership (grant number NE/L002558/1). A. P. Schurer and G.Hegerl. were supported by NERC under the Belmont forum, Grant PacMedy (NE/P006752/1). The authors acknowledge the World Climate Research Program's Working Group on Coupled Modeling, which is responsible for CMIP, and thank all the climate modeling groups for producing and making available their model output. The authors acknowledge the Northern Hemisphere Tree-Ring Network Development (N-TREND) and the Past Global Changes (PAGES) project for providing publicly available data.

References

Alley, R. B., Brook, E. J., & Anandakrishnan, S. (2002). A northern lead in the orbital band: north–south phasing of Ice-Age events. *Quaternary Science Reviews*, *21*(1-3), 431–441. https://doi.org/10.1016/s0277-3791(01)00072-5

Anchukaitis, K., Wilson, R., Briffa, K. R., Büntgen, U., Cook, E. R., D'Arrigo, R., et al. (2017). Last millennium Northern Hemisphere summer temperatures from tree rings: Part II, spatially resolved reconstructions. *Quaternary Science Reviews*, *163*, 1–22. https://doi.org/10.1016/j.quascirev.2017.02.020

Bathen, K. H. (1972). On the seasonal changes in the depth of the mixed layer in the north Pacific Ocean. *Journal of Geophysical Research*, *77*(36), 7138–7150. https://doi.org/10.1029/jc077i036p07138

Berger, A., & Loutre, M. F. (1991). Insolation values for the climate of the last 10 million years. *Quaternary Science Reviews*, *10*(4), 297–317. https://doi.org/10.1016/0277-3791(91)90033-q

Björklund, J. A., Gunnarson, B. E., Seftigen, K., Esper, J., & Linderholm, H. W. (2014). Blue intensity and density from northern Fennoscandian tree rings, exploring the potential to improve summer temperature reconstructions with earlywood information. *Climate of the Past*, *10*(2), 877–885. https://doi.org/10.5194/cp-10-877-2014

Björklund, J., Seftigen, K., Schweingruber, F., Fonti, P., von Arx, G., Bryukhanova, M. V., et al. (2017). Cell size and wall dimensions drive distinct variability of earlywood and latewood density in Northern Hemisphere conifers. *New Phytologist*, *216*(3), 728–740. https://doi.org/10.1111/nph.14639

Böhm, R., Jones, P. D., Hiebl, J., Frank, D., Brunetti, M., & Maugeri, M. (2010). The early instrumental warm-bias: a solution for long central European temperature series 1760–2007. *Climatic Change*, *101*(1-2), 41–67. https://doi.org/10.1007/s10584-009-9649-4

Braconnot, P., Harrison, S. P., Kageyama, M., Bartlein, P. J., Masson-Delmotte, V., Abe-Ouchi, A., et al. (2012). Evaluation of climate models using palaeoclimatic data. *Nature Climate Change*, *2*, (6), 417–424. https://doi.org/10.1038/nclimate1456

Briffa, K. R (2000). Annual climate variability in the Holocene: interpreting the message of ancient trees. *Quaternary Science Reviews*, *19*(1-5), 87–105. https://doi.org/10.1016/s0277-3791(99)00056-6

Cook, E. R., Esper, J., & D'Arrigo, R. D. (2004). Extra-tropical Northern Hemisphere land temperature variability over the past 1000 years. *Quaternary Science Reviews*, *23*(20–22), 2063–2074. https://doi.org/10.1016/j.quascirev.2004.08.013

D'Arrigo, R., Wilson, R., & Jacoby, G. (2006). On the long-term context for late twentieth century warming. *Journal of Geophysical Research*, *111*(D3), D03103.1–D03103.12. https://doi.org/10.1029/2005jd006352

Donohoe, A., Dawson, E., McMurdie, L., Battisti, D. S., & Rhines, A. (2020). Seasonal Asymmetries in the Lag between Insolation and Surface Temperature. *Journal of Climate*, *33*(10), 3921–3945. https://doi.org/10.1175/jcli-d-19-0329.1

Dufresne, J.-L., Foujols, M.-A., Denvil, S., Caubel, A., Marti, O., Aumont, O., et al. (2013). Climate change projections using the IPSL-CM5 Earth System Model: from CMIP3 to CMIP5. *Climate Dynamics*, *40*(9-10), 2123–2165. https://doi.org/10.1007/s00382-012-1636-1

Esper, J. (2002). Low-frequency signals in long tree-ring chronologies for reconstructing past temperature variability. *Science*, *295*(5563), 2250–2253. https://doi.org/10.1126/science.1066208

Esper, J., Frank, D. C., & Wilson, R. J. S. (2004). Climate reconstructions: Low-frequency ambition and high-frequency ratification. *Eos, Transactions American Geophysical Union*, *85*(12), 113. https://doi.org/10.1029/2004eo120002

Fischer, N., & Jungclaus, J. H. (2011). Evolution of the seasonal temperature cycle in a transient Holocene simulation: orbital forcing and sea-ice. *Climate of the Past*, *7*(4), 1139–1148. https://doi.org/10.5194/cp-7-1139-2011

Frank, D., Büntgen, U., Böhm, R., Maugeri, M., & Esper, J. (2007). Warmer early instrumental measurements versus colder reconstructed temperatures: shooting at a moving target. *Quaternary Science Reviews*, *26*(25-28), 3298–3310. https://doi.org/10.1016/j.quascirev.2007.08.002

Fuentes, M., Salo, R., Björklund, J., Seftigen, K., Zhang, P., Gunnarson, B., et al. (2018). A 970-year-long summer temperature reconstruction from Rogen, west-central Sweden, based on blue intensity from tree rings. *The Holocene*, *28*(2), 254–266. https://doi.org/10.1177/0959683617721322

Hays, J. D., Imbrie, J., & Shackleton, N. J. (1976). Variations in the Earth's Orbit: Pacemaker of the Ice Ages. *Science*, *194*(4270), 1121–1132. https://doi.org/10.1126/science.194.4270.1121

Esper, J., Frank, D. C., Timonen, M., Zorita, E., Wilson, R. J. S., Luterbacher, J., et al. (2012). Orbital forcing of tree-ring data. *Nature Climate Change*, *2*(12), 862–866. https://doi.org/10.1038/nclimate1589

Esper, J., Wilson, R. J., Frank, D. C., Moberg, A., Wanner, H., & Luterbacher, J. (2005). Climate: Past ranges and future changes. *Quaternary Science Reviews*, *24*(20–21), 2164–2166. https://doi.org/10.1016/j.quascirev.2005.07.001

Giorgetta, M. A., Jungclaus, J., Reick, C. H., Legutke, S., Bader, J., Böttinger, M., et al. (2013). Climate and carbon cycle changes from 1850 to 2100 in MPI-ESM simulations for the Coupled Model Intercomparison Project phase 5. *Journal of Advances in Modeling Earth Systems*, *5*(3), 572–597. https://doi.org/10.1002/jame.20038

Harris, I., Jones, P. D., Osborn, T. J., & Lister, D. H. (2014). Updated high-resolution grids of monthly climatic observations - the CRU TS3.10 Dataset. *International Journal of Climatology*, *34*(3), 623–642. https://doi.org/10.1002/joc.3711

Klippel, L., St. George, S., Büntgen, U., Krusic, P. J., & Esper, J. (2020). Differing pre-industrial cooling trends between tree rings and lower-resolution temperature proxies. *Climate of the Past*, *16*(2), 729–742. https://doi.org/10.5194/cp-16-729-2020

Imbrie, J., Boyle, E. A., Clemens, S. C., Duffy, A., Howard, W. R., Kukla, G., et al. (1992). On the Structure and Origin of Major Glaciation Cycles 1. Linear Responses to Milankovitch Forcing. *Paleoceanography*, *7*(6), 701–738. https://doi.org/10.1029/92pa02253

Kaufman, D. S., Schneider, D. P., McKay, N. P., Ammann, C. M., Bradley, R. S., Briffa, K. R., et al., (2009). Recent Warming Reverses Long-Term Arctic Cooling. *Science*, *325*(5945), 1236–1239. https://doi.org/10.1126/science.1173983

Kawamura, K., Parrenin, F., Lisiecki, L., Uemura, R., Vimeux, F., Severinghaus, J. P., et al. (2007). Northern Hemisphere forcing of climatic cycles in Antarctica over the past 360,000 years. *Nature*, *448*(7156), 912–916. https://doi.org/10.1038/nature06015

Landrum, L., Otto-Bliesner, B. L., Wahl, E. R., Conley, A., Lawrence, P. J., Rosenbloom, N., & Teng, H. (2013). Last millennium climate and its variability in CCSM4. *Journal of Climate*, *26*(4), 1085–1111. https://doi.org/10.1175/jcli-d-11-00326.1

Laskar, J. (1986). Secular terms of classical planetary theories using the results of general theory. *Astronomy and astrophysics*, *157*, 59–70.

Laskar, J. (1988). Secular evolution of the solar system over 10 million years. *Astronomy and Astrophysics*, *198*, 341–362.

Laskar, J., Robutel, P., Joutel, F., Gastineau, M., Correia, A. C. M., & Levrard, B. (2004). A long-term numerical solution for the insolation quantities of the Earth. *Astronomy & Astrophysics*, *428*(1), 261–285. https://doi.org/10.1051/0004-6361:20041335

Ljungqvist, F. C., Zhang, Q., Brattström, G., Krusic, P. J., Seim, A., Li, Q., et al. (2019). Centennial-Scale Temperature Change in Last Millennium Simulations and Proxy-Based Reconstructions. *Journal of Climate*, *32*(9), 2441–2482. https://doi.org/10.1175/jcli-d-18-0525.1

Lücke, L. J., Hegerl, G. C., Schurer, A. P., & Wilson, R. (2019). Effects of memory biases on variability of temperature reconstructions. *Journal of Climate*, *32*(24), 8713–8731. https://doi.org/10.1175/jcli-d-19-0184.1

Masson-Delmotte, V., Schulz, M., Abe-Quichi, A., Beer, J., Ganopolski, A., Gonzalez Rouco, J. F., et al. (2013). Information from Paleoclimate Archives. *Climate Change 2013: The Physical Science Basis. Contribution of Working Group I to the Fifth Assessment Report of the Intergovernmental Panel on Climate Change*. Cambridge, United Kingdom and New York, NY, USA: Cambridge University Press.

McKay, N. P., & Kaufman, D. S. (2014). An extended arctic proxy temperature database for the past 2,000 years. *Scientific Data*, *1*(1), 140026. https://doi.org/10.1038/sdata.2014.26

Melvin, T. M., Grudd, H., & Briffa, K. R. (2012). Potential bias in 'updating' tree-ring chronologies using regional curve standardization: Re-processing 1500 years of Torneträsk density and ring-width data. *The Holocene*, *23*(3), 364–373. https://doi.org/10.1177/0959683612460791

Milankovitch, M. M. (1941). Kanon der Erdbestrahlung und seine Anwendung auf das Eiszeitenproblem. *Koniglich Serbische Akademice Beograd Special Publication*, *132*,

Neukom, R., Barboza, L. A., Erb, M. P., Shi, F., Emile-Geay, J., Evans, M. N., et al. (2019). Consistent multidecadal variability in global temperature reconstructions and simulations over the common era. *Nature Geoscience*, *2*(8), 643–649. https://doi.org/10.1038/s41561-019-0400-0

Osborn, T. J., & Jones, P. D. (2014). The CRUTEM4 land-surface air temperature data set: construction, previous versions and dissemination via Google Earth. *Earth System Science Data*, *6*(1), 61–68. https://doi.org/10.5194/essd-6-61-2014

Otto-Bliesner, B. L., Brady, E. C., Fasullo, J., Jahn, A., Landrum, L., Stevenson, S., et al. (2016). Climate Variability and Change since 850 CE: An Ensemble Approach with the Community Earth System Model. *Bulletin of the American Meteorological Society*, *97*(5), 735–754. https://doi.org/10.1175/bams-d-14-00233.1

PAGES2k (2013). Continental-scale temperature variability during the past two millennia. *Nature Geoscience*, *6*(5), 339–346. https://doi.org/10.1038/ngeo1797

Parrenin, F., & Paillard, D. (2003). Amplitude and phase of glacial cycles from a conceptual model. *Earth and Planetary Science Letters*, *214*(1-2), 243–250. https://doi.org/10.1016/s0012-821x(03)00363-7

Phipps, S. J., McGregor, H. V., Gergis, J., Gallant, A. J. E., Neukom, R., Stevenson, S., et al. (2013). Paleoclimate Data–Model Comparison and the Role of Climate Forcings over the Past 1500 Years*. *Journal of Climate*, *26*(18), 6915–6936. https://doi.org/10.1175/jcli-d-12-00108.1

Phipps, S. J., McGregor, H. V., Gergis, J., Gallant, A. J. E., Neukom, R., Stevenson, S., et al. (2013). Paleoclimate Data–Model Comparison and the Role of Climate Forcings over the Past 1500 Years*. *Journal of Climate*, *26*(18), 6915–6936. https://doi.org/10.1175/jcli-d-12-00108.1

Phipps, S. J., Rotstayn, L. D., Gordon, H. B., Roberts, J. L., Hirst, A. C., & Budd, W. F. (2011). The CSIRO Mk3L climate system model version 1.0 – Part 1: Description and evaluation. *Geoscientific Model Development*, *4*(2), 483–509. https://doi.org/10.5194/gmd-4-483-2011

Phipps, S. J., Rotstayn, L. D., Gordon, H. B., Roberts, J. L., Hirst, A. C., & Budd, W. F. (2012). The CSIRO Mk3L climate system model version 1.0 – Part 2: Response to external forcings. *Geoscientific Model Development*, *5*(3), 649–682. https://doi.org/10.5194/gmd-5-649-2012

Prescott, J. A., & Collins, J. A. (1951). The lag of temperature behind solar radiation. *Quarterly Journal of the Royal Meteorological Society*, *77*(331), 121–126. https://doi.org/10.1002/qj.49707733112

Raymo, M. E. (1997). The timing of major climate terminations. *Paleoceanography*, *12*(4), 577–585. https://doi.org/10.1029/97pa01169

Rydval, M., Larsson, L.-Å., McGlynn, L., Gunnarson, B. E., Loader, N. J., Young, G. H. F., & Wilson, R. (2014). Blue intensity for dendroclimatology: Should we have the blues? Experiments from Scotland. *Dendrochronologia*, *32*(3), 191–204. https://doi.org/10.1016/j.dendro.2014.04.003

Schneider, L., Smerdon, J. E., Büntgen, U., Wilson, R. J. S., Myglan, V. S., Kirdyanov, A. V., & Esper, J. (2015). Revising midlatitude summer temperatures back to A.D. 600 based on a wood density network. *Geophysical Research Letters*, *42*(11), 4556–4562. https://doi.org/10.1002/2015gl063956

Schmidt, G. A., Jungclaus, J. H., Ammann, C. M., Bard, E., Braconnot, P., Crowley, T. J., et al. (2011). Climate forcing reconstructions for use in PMIP simulations of the last millennium (v1.0). *Geoscientific Model Development*, *4*(1), 33–45. https://doi.org/10.5194/gmd-4-33-2011

Schmidt, G. A., Jungclaus, J. H., Ammann, C. M., Bard, E., Braconnot, P., Crowley, T. J., et al. (2012). Climate forcing reconstructions for use in PMIP simulations of the Last Millennium (v1.1). *Geoscientific Model Development*, *5*(1), 185–191. https://doi.org/10.5194/gmd-5-185-2012

Schmidt, G. A., Kelley, M., Nazarenko, L., Ruedy, R., Russell, G. L., Aleinov, I., et al. (2014). Configuration and assessment of the GISS ModelE2 contributions to the CMIP5 archive. *Journal of Advances in Modeling Earth Systems*, *6*(1), 141–184. https://doi.org/10.1002/2013ms000265

Schurer, A. P., Hegerl, G. C., Mann, M. E., Tett, S. F. B., & Phipps, S. J. (2013). Separating Forced from Chaotic Climate Variability over the Past Millennium. *Journal of Climate*, *26*(18), 6954–6973. https://doi.org/10.1175/jcli-d-12-00826.1

Schurer, A. P., Tett, S. F. B., & Hegerl, G. C. (2014). Small influence of solar variability on climate over the past millennium. *Nature Geoscience*, *7*(2), 104–108. https://doi.org/10.1038/ngeo2040

Taylor, K. E., Stouffer, R. J., & Meehl, G. A. (2012). An Overview of CMIP5 and the Experiment Design. *Bulletin of the American Meteorological Society*, *93*(4), 485–498. https://doi.org/10.1175/bams-d-11-00094.1

Wanner, H., Beer, J., Bütikofer, J., Crowley, T. J., Cubasch, U., Flückiger, J., et al. (2008). Mid- to Late Holocene climate change: an overview. *Quaternary Science Reviews*, *27*(19-20), 1791–1828. https://doi.org/10.1016/j.quascirev.2008.06.013

Wilson, R., Anchukaitis, K., Briffa, K. R., Büntgen, U., Cook, E., D'Arrigo, R., et al. (2016). Last millennium Northern Hemisphere summer temperatures from tree rings: Part I: The long term context. *Quaternary Science Reviews*, *134*, 1–18. https://doi.org/10.1016/j.quascirev.2015.12.005

Wilson, R., D'Arrigo, R., Buckley, B., Büntgen, U., Esper, J., Frank, D., et al. (2007). A matter of divergence: Tracking recent warming at hemispheric scales using tree ring data. *Journal of Geophysical Research*, *112*(D17), D17103. https://doi.org/10.1029/2006jd008318

Zhang, P., Linderholm, H. W., Gunnarson, B. E., Björklund, J., & Chen, D. (2015). 1200 years of warm-season temperature variability in central Fennoscandia inferred from tree-ring density. *Climate of the Past Discussions*, *11*(1), 489–519. https://doi.org/10.5194/cpd-11-489-2015

References From the Supporting Information

Anchukaitis, K., D'Arrigo, R., Andreu-Hayles, L., Frank, D., Verstege, A., Curtis, A., et al. (2013). Tree-ring-reconstructed summer temperatures from Northwestern North America during the last nine centuries. *Journal of Climate*, *26*(10), 3001–3012. https://doi.org/10.1175/jcli-d-11-00139.1

Biondi, F., Perkins, D. L., Cayan, D. R., & Hughes, M. K. (1999). July temperature during the second millennium reconstructed from Idaho tree rings. *Geophysical Research Letters*, *26*(10), 1445–1448. https://doi.org/10.1029/1999gl900272

Bird, B. W., Abbott, M. B., Finney, B. P., & Kutchko, B. (2008). A 2000 year varve-based climate record from the central brooks range, Alaska. *Journal of Paleolimnology*, *41*(1), 25–41. https://doi.org/10.1007/s10933-008-9262-y

Briffa, K. R., Melvin, T. M., Osborn, T. J., Hantemirov, R. M., Kirdyanov, A. V., Mazepa, V. S., et al. (2013). Reassessing the evidence for tree-growth and inferred temperature change during the common era in Yamalia, Northwest Siberia. *Quaternary Science Reviews*, *72*, 83–107. https://doi.org/10.1016/j.quascirev.2013.04.008

Briffa, K. R., Shishov, V. V., Melvin, T. M., Vaganov, E. A., Grudd, H., Hantemirov, R. M., et al. (2007). Trends in recent temperature and radial tree growth spanning 2000 years across Northwest Eurasia. *Philosophical Transactions of the Royal Society B: Biological Sciences*, *363*(1501), 2269–2282. https://doi.org/10.1098/rstb.2007.2199

Büntgen, U., Frank, D. C., Nievergelt, D., & Esper, J. (2006). Summer temperature variations in the European Alps, a.d.755-2004. *Journal of Climate*, *19*(21), 5606–5623. https://doi.org/10.1175/jcli3917.1

Büntgen, U., Kyncl, T., Ginzler, C., Jacks, D. S., Esper, J., Tegel, W., et al. (2013). Filling the Eastern European gap in millennium-long temperature reconstructions. *Proceedings of the National Academy of Sciences*, *110*(5), 1773–1778. https://doi.org/10.1073/pnas.1211485110

Cook, T. L., Bradley, R. S., Stoner, J. S., & Francus, P. (2008). Five thousand years of sediment transfer in a high arctic watershed recorded in annually laminated sediments from lower Murray Lake, Ellesmere Island, Nunavut, Canada. *Journal of Paleolimnology*, *41*(1), 77–94. https://doi.org/10.1007/s10933-008-9252-0

Cook, E. R., D'Arrigo, R. D., & Mann, M. E. (2002). A well-verified, multiproxy reconstruction of the winter North Atlantic oscillation index since a.d.1400*. *Journal of Climate*, *15*(13), 1754–1764.

Cook, E. R., Krusic, P. J., Anchukaitis, K., Buckley, B. M., Nakatsuka, T., & Sano, M. (2012). Tree-ring reconstructed summer temperature anomalies for temperate East Asia since 800 C. *E. Climate Dynamics*, *41*(11–12), 2957–2972. https://doi.org/10.1007/s00382-012-1611-x

Dansgaard, W., Johnsen, S. J., Moller, J., & Langway, C. C. (1969). One thousand centuries of climatic record from camp century on the Greenland ice sheet. *Science*, *166*(3903), 377–380. https://doi.org/10.1126/science.166.3903.377

Davi, N. (2003). Boreal temperature variability inferred from maximum latewood density and tree-ring width data, Wrangell Mountain region, Alaska. *Quaternary Research*, *7*, 63–111. https://doi.org/10.1016/s0033-5894(03)00115-7

Davi, N., D'Arrigo, R., Jacoby, G., Cook, E., Anchukaitis, K., Nachin, B., et al. (2015). A long-term context (931–2005 C.E.) for rapid warming over Central Asia. *Quaternary Science Reviews*, *121*, 89–97. https://doi.org/10.1016/j.quascirev.2015.05.020

Divine, D., Isaksson, E., Martma, T., Meijer, H. A., Moore, J., Pohjola, V., et al. (2011). Thousand years of winter surface air temperature variations in Svalbard and Northern Norway reconstructed from ice-core data. *Polar Research*, *30*(1), 7379. https://doi.org/10.3402/polar.v30i0.7379

D'Arrigo, R., Buckley, B., Kaplan, S., & Woollett, J. (2003). Interannual to multidecadal modes of Labrador climate variability inferred from tree rings. *Climate Dynamics*, *20*(2), 219–228. https://doi.org/10.1007/s00382-002-0275-3

D'Arrigo, R., Jacoby, G., Buckley, B., Sakulich, J., Frank, D., Wilson, R., et al. (2009). Tree growth and inferred temperature variability at the North American Arctic treeline. *Global and Planetary Change*, *65*(1–2), 71–82. https://doi.org/10.1016/j.gloplacha.2008.10.011

D'Arrigo, R., Mashig, E., Frank, D., Jacoby, G., & Wilson, R. (2004). Reconstructed warm season temperatures for Nome, Seward Peninsula, Alaska. *Geophysical Research Letters*, *31*(9). n/a–n/a. https://doi.org/10.1029/2004gl019756

D'Arrigo, R., Mashig, E., Frank, D., Wilson, R., & Jacoby, G. (2005). Temperature variability over the past millennium inferred from Northwestern Alaska tree rings. *Climate Dynamics*, *24*(2–3), 227–236. https://doi.org/10.1007/s00382-004-0502-1

D'Arrigo, R., Wilson, R., & Anchukaitis, K. (2013). Volcanic cooling signal in tree ring temperature records for the past millennium. *Journal of Geophysical Research: Atmosphere*, *118*(16), 9000–9010. https://doi.org/10.1002/jgrd.50692

D'Arrigo, R., Wilson, R., Wiles, G., Anchukaitis, K., Solomina, O., Davi, N., et al. (2014). Tree-ring reconstructed temperature index for Coastal Northern Japan: implications for Western North Pacific variability. *International Journal of Climatology*, *35*(12), 3713–3720. https://doi.org/10.1002/joc.4230

Esper, J., Duethorn, E., Krusic, P. J., Timonen, M., & Buentgen, U. (2014). Northern European summer temperature variations over the common era from integrated tree-ring density records. *Journal of Quaternary Science*, *29*(5), 487–494. https://doi.org/10.1002/jqs.2726

Frank, D. C., Esper, J., Raible, C. C., Büntgen, U., Trouet, V., Stocker, B., & Joos, F. (2010). Ensemble reconstruction constraints on the global carbon cycle sensitivity to climate. *Nature*, *463*(7280), 527–530. https://doi.org/10.1038/nature08769

Gennaretti, F., Arseneault, D., Nicault, A., Perreault, L., & Begin, Y. (2014). Volcano-induced regime shifts in millennial tree-ring chronologies from Northeastern North America. *Proceedings of the National Academy of Sciences*, *111*(28), 10077–10082. https://doi.org/10.1073/pnas.1324220111

Grootes, P. M., & Stuiver, M. (1997). Oxygen 18/16 variability in Greenland snow and ice with 10-3- to 105-year time resolution. *Journal of Geophysical Research*, *102*(C12), 26455–26470. https://doi.org/10.1029/97jc00880

Gunnarson, B. E., Linderholm, H. W., & Moberg, A. (2010). Improving a tree-ring reconstruction from West-Central Scandinavia: 900 years of warm-season temperatures. *Climate Dynamics*, *36*(1–2), 97–108. https://doi.org/10.1007/s00382-010-0783-5

Helama, S., Fauria, M. M., Mielikainen, K., Timonen, M., & Eronen, M. (2010). Sub-Milankovitch solar forcing of past climates: Mid and Late Holocene perspectives. *The Geological Society of America Bulletin*, *122*(11–12), 1981–1988. https://doi.org/10.1130/b30088.1

Helama, S., Vartiainen, M., Holopainen, J., Mäkelä, H., Kolström, T., & Meriläinen, J. (2014). A paleotemperature record for the Finnish Lakeland based on microdensitometric variations in tree rings. *Geochronometria*, *41*(3), 265–277. https://doi.org/10.2478/s13386-013-0163-0

Hughes, M. K., Vaganov, E. A., Shiyatov, S., Touchan, R., & Funkhouser, G. (1999). Twentieth-century summer warmth in Northern Yakutia in a 600-year context. *The Holocene*, *9*(5), 629–634. https://doi.org/10.1191/095968399671321516

Isaksson, E., Divine, D., Kohler, J., Martma, T., Pohjola, V., Motoyama, H., & Watanabe, O. (2005). Climate oscillations as recorded in Svalbard ice core ω18o records between ad 1200 and 1997. *Geografiska Annaler – Series A: Physical Geography*, *87*(1), 203–214. https://doi.org/10.1111/j.0435-3676.2005.00253.x

Jacoby, G. C., Lovelius, N. V., Shumilov, O. I., Raspopov, O. M., Karbainov, J. M., & Frank, D. C. (2000). Long-term temperature trends and tree growth in the Taymir region of Northern Siberia. *Quaternary Research*, *53*(03), 312–318. https://doi.org/10.1006/qres.2000.2130

Kirchhefer, A. J. (2001). Reconstruction of summer temperatures from tree-rings of Scots pine (Pinus Sylvestris L.) in coastal Northern Norway. *The Holocene*, *11*(1), 41–52. https://doi.org/10.1191/095968301670181592

Klesse, S., Ziehmer, M., Rousakis, G., Trouet, V., & Frank, D. (2014). Synoptic drivers of 400 years of summer temperature and precipitation variability on Mt. Olympus, Greece. *Climate Dynamics*, *45*(3–4), 807–824. https://doi.org/10.1007/s00382-014-2313-3

Lamoureux, S., & Bradley, R. (1996). A late Holocene varved sediment record of environmental change from northern Ellesmere Island, Canada. *Journal of Paleolimnology*, *16*(2), 239–255. https://doi.org/10.1007/bf00176939

Larsen, D. J., Miller, G. H., Geirsdóttir, Á., & Thordarson, T. (2011). A 3000-year varved record of glacier activity and climate change from the proglacial Lake Hvítárvatn, Iceland. *Quaternary Science Reviews*, *30*(19–20), 2715–2731. https://doi.org/10.1016/j.quascirev.2011.05.026

Liñán, I. D., Büntgen, U., González-Rouco, F., Zorita, E., Montávez, J. P., Gómez-Navarro, J. J., et al. (2012). Estimating 750 years of temperature variations and uncertainties in the Pyrenees by tree-ring reconstructions and climate simulations. *Climate of the Past*, *8*(3), 919–933. https://doi.org/10.5194/cp-8-919-2012

Linderholm, H. W., Björklund, J., Seftigen, K., Gunnarson, B. E., & Fuentes, M. (2014). Fennoscandia revisited: A spatially improved tree-ring reconstruction of summer temperatures for the last 900 years. *Climate Dynamics*, *45*(3–4), 933–947. https://doi.org/10.1007/s00382-014-2328-9

Loso, M. G., Anderson, R. S., Anderson, S. P., & Reimer, P. J. (2006). A 1500-year record of temperature and glacial response inferred from varved Iceberg lake, Southcentral Alaska. *Quaternary Research*, *66*(1), 12–24. https://doi.org/10.1016/j.yqres.2005.11.007

Luckman, B., & Wilson, R. (2005). Summer temperatures in the Canadian rockies during the last millennium: A revised record. *Climate Dynamics*, *24*(2–3), 131–144. https://doi.org/10.1007/s00382-004-0511-0

Matskovsky, V. V., & Helama, S. (2014). Testing long-term summer temperature reconstruction based on maximum density chronologies obtained by reanalysis of tree-ring data sets from Northernmost Sweden and Finland. *Climate of the Past*, *10*(4), 1473–1487. https://doi.org/10.5194/cp-10-1473-2014

McCarroll, D., Loader, N. J., Jalkanen, R., Gagen, M. H., Grudd, H., Gunnarson, B. E., et al. (2013). A 1200-year multiproxy record of tree growth and summer temperature at the Northern Pine Forest limit of Europe. *The Holocene*, *23*(4), 471–484. https://doi.org/10.1177/0959683612467483

Meko, D. (1997). Dendroclimatic reconstruction with time varying predictor subsets of tree indices. *Journal of Climate*, *10*(4), 687–696.

Moore, J., Hughen, K., Miller, G., & Overpeck, J. (2001). Little ice age recorded in summer temperature reconstruction from vared sediments of Donard lake, Baffin Island, Canada. *Journal of Paleolimnology*, *25*(4), 503–517. https://doi.org/10.1023/a:1011181301514

Rydval, M., Loader, N. J., Gunnarson, B. E., Druckenbrod, D. L., Linderholm, H. W., Moreton, S. G., et al. (2017). Reconstructing 800 years of summer temperatures in Scotland from tree rings. *Climate Dynamics*, *49*(9–10), 2951–2974. https://doi.org/10.1007/s00382-016-3478-8

Schwager, M. (2000). *Ice core analysis on the spatial and temporal variability of temperature and precipitation during the late Holocene in North Greenland;eisbohrkernuntersuchungen zur raeumlichen und zeitlichen variabilitaet von temperatur und niederschlagsrate im spaetholozaen in nordgroenland*.

Szeicz, J. M., & MacDonald, G. M. (1995). Dendroclimatic reconstruction of summer temperatures in northwestern Canada since A.D. 1638 based on age-dependent modeling. *Quaternary Research*, *44*(02), 257–266. https://doi.org/10.1006/qres.1995.1070

Thomas, E. K., & Briner, J. P. (2008). Climate of the past millennium inferred from varved proglacial lake sediments on Northeast Baffin Island, Arctic Canada. *Journal of Paleolimnology*, *41*(1), 209–224. https://doi.org/10.1007/s10933-008-9258-7

Zhang, P., Linderholm, H. W., Gunnarson, B. E., Björklund, J., & Chen, D. (2015). 1200 years of warm-season temperature variability in central Fennoscandia inferred from tree-ring density. *Climate of the Past Discussions*, *11*(1), 489–519. https://doi.org/10.5194/cpd-11-489-2015